



# Regulation of protein phosphatase 2A by ARPP-16 and MAST kinase in striatal medium spiny neurons

MUSANTE V.<sup>1</sup>, ANDRADE E.<sup>2</sup>, HORIUCHI A.<sup>3</sup>, GREENGARD P.<sup>3</sup>, NAIRN A.C.<sup>1,3</sup>

<sup>1</sup>Dept. of Psychiatry, Yale Univ. Sch. of Med., New Haven, CT; <sup>2</sup>Lab. of Mol. Biol., <sup>3</sup>Lab. of Mol. and Cell. Neurosci., Rockefeller Univ., New York, NY

## INTRODUCTION

Dopamine plays an important modulatory role in the central nervous system, helping to control critical aspects of motor function and reward learning. Alterations in normal dopaminergic neurotransmission underlay multiple neurological diseases, including schizophrenia, Huntington's disease and Parkinson's disease, and the addictive actions of drugs of abuse.

In striatal medium spiny neurons, the effects of dopamine are mediated by the phosphoproteins DARPP-32 and RCS, two regulators of serine/threonine phosphatases PP1 and PP2B, respectively, which are controlled by cAMP-dependent phosphorylation. Another protein kinase A (PKA) substrate that is enriched in striatum is ARPP-16. Member of ARPP family (ARPP-16, ARPP-19 and endosulfine) are highly conserved during evolution, and while ARPP-19 and endosulfine show a ubiquitous tissue distribution, ARPP-16 is highly enriched in medium spiny neurons (Girault et al., J. Neurosci., 1990).

Our protein interaction studies have shown that ARPP-16 binds to the A subunit of the serine/threonine protein phosphatase 2A (PP2A), a heterotrimeric assembly of a core catalytic/regulatory subunit AC dimer, together with a variable B subunit that controls localization and substrate specificity.

Previous studies have identified two phosphorylation sites in ARPP-16, one near the C-terminus that is phosphorylated by PKA, while a second site, Ser46 (Ser62 in ARPP-19) located in a central region, has not been well characterized (Dubouva et al., J Neurochem, 2001).

Recent studies in Xenopus oocytes have demonstrated that ARPP-19 or endosulfine, when phosphorylated by Xenopus Kinase, inhibits PP2A during the mitosis (Mochida et al., Science 2010, Gharby-Ayachi et al., Science 2010). As microtubule associated kinases (MAST) are the mammalian homologues of Greatwall and one isoform (MAST3) is enriched in the striatum.

We tested, *in vitro* and by recombinant protein expression in HEK cells, the ability of these MAST kinases to phosphorylate ARPP-16. Our results show MAST is able to phosphorylate ARPP-16 at Ser46 and this phosphorylation significantly increases the ability of ARPP to inhibit PP2A. Moreover MAST-phosphorylated ARPP-16 exhibits specifically for the trimeric form of PP2A compared to its dimeric form, and the inhibition depends on the co-assembled B subunit.

Ser46 of ARPP-16 is phosphorylated to very high level basally, indicating phospho-ARPP-16 acts to control PP2A activity. Experiments are in progress to characterize the possible effect of PKA in the MAST-mediated phosphorylation of ARPP-16 and regulation of PP2A.

**Take together our data suggest, like DARPP-32 and RCS, ARPP-16 controls the activity of protein dephosphorylation in striatal neurons.**

## METHODS

**Cell line culture:** HEK 293-T cells were grown on un-coated plates in DMEM (Invitrogen), supplemented with 10% FBS.

**GST pull-downs:** His-ARPP-16 was immobilized onto 80  $\mu$ l sample (of 50/50 slurry) Talon metal affinity resin Clontech Laboratory Inc. Mountain View, CA). Increasing amounts of purified PP2A-A (0, 20 ng, 40 ng, 200 ng, or 400 ng) were added to the beads and samples were incubated for 1 hr at 4°C with rotation. As a control, 40 ng PP2A-A was added to beads with no His-ARPP-16 immobilized.

**Plasmids and Transfection:** MAST3-HA, ARPP-16-HA, Bala-FLAG, B560-FLAG and PR72-FLAG constructs were transfected in HEK293 cells with Lipofectamine 2000 (Invitrogen) in Opti-MEM media (Invitrogen). A Protein expression was assayed at least 24 hr later.

**ARPP-16 *in vitro* phosphorylation:** Recombinant ARPP-16 fused to beta tag was expressed in Escherichia coli (BL21) and purified using Ni-NTA-Agarose (Qiagen). Purified His-ARPP-16 (1  $\mu$ M) has been resuspended in 100  $\mu$ l of phosphorylation buffer (50 mM HEPES pH 7.4, 10 mM MgCl<sub>2</sub>) in presence of 200  $\mu$ M ATP (Sigma) or 1 mM  $\gamma$ -ATP (Roche) and incubated at 37°C for different time with immunoprecipitated MAST3 kinase.

**Immunoprecipitation and Malachite green Phosphatase assay:** Lysates of transfected cells were incubated with 50  $\mu$ l (50% slurry) of His-FLAG conjugated agarose beads for 2 h at 4°C. Immunocomplexes were washed three times in lysis buffer without phosphatase inhibitors and two times in PP2A reaction buffer (50 mM Tris-HCl, pH 7, 100  $\mu$ M CaCl<sub>2</sub>). Immunocomplexes for B560- or PR72- PP2A trimers or purified PP2A-A dimer (0.01  $\mu$ M, Millipore) were resuspended in 100  $\mu$ l of PP2A reaction buffer and incubated with or without ARPP-16 or  $\gamma$ -ATP-phosphorylated ARPP-16 (50 nM, 100 nM, 1  $\mu$ M) for 10 min at 37°C in presence of 500  $\mu$ M Threonine phosphatidate (K-R-p-174-R). The phosphatase activity was measured by malachite green assay (Millipore).

**DARPP-32 *in vitro* phosphorylation and PP2A activity assay:** recombinant purified DARPP-32 (200  $\mu$ g) was phosphorylated by CKII at 30°C for 1 hour. In buffer containing 50 mM Tris-HCl, pH 7.5, 150 mM KCl, 10 mM magnesium acetate and 200  $\mu$ M  $\gamma$ -ATP. Proteins were precipitated in 100% Trichloroacetic acid (TCA) and after centrifugation the pellet was resuspended and dialyzed in 20 mM Tris-HCl pH 7.5, 5 mM  $\beta$ -mercapto-ethanol. For the PP2A assay, different PP2A heterotrimer were incubated with or without ARPP-16 or  $\gamma$ -ATP-phosphorylated ARPP-16 (200 nM) in presence of 75  $\mu$ g of [<sup>32</sup>P]-DARPP-32 for 10 minutes at 30°C. Free [<sup>32</sup>P] label was measured by scintillation after precipitation of [<sup>32</sup>P]-phosphorylation of DARPP-32.

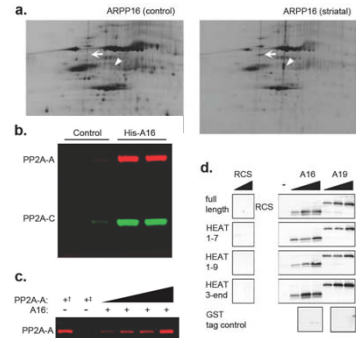
**Striatal slice preparation:** Striatal slices from 6-week old mice were prepared as described with slight procedural modifications (Nairn et al., 1997). The brains were rapidly removed and placed in ice-cold, oxygenated Krebs-HCO<sub>3</sub> buffer (124 mM NaCl, 4 mM KCl, 26 mM NaHCO<sub>3</sub>, 1.5 mM CaCl<sub>2</sub>, 1.25 mM KH<sub>2</sub>PO<sub>4</sub>, 1.5 mM MgSO<sub>4</sub>, 10 mM  $\beta$ -D-glucose, pH 7.4). Coronal slices (350  $\mu$ m) were prepared using a vibrating blade microtome (VT1000S, Leica Microsystems). Strata were dissected from the slices and then placed in a polypropylene incubation tube with 2 ml of fresh, oxygenated Krebs-HCO<sub>3</sub> buffer and allowed to recover for 30 min with constant oxygenation with 95% O<sub>2</sub>/5% CO<sub>2</sub> at 30°C followed by another 30 min of recovery with adenosine deaminase added to fresh Krebs-HCO<sub>3</sub> buffer.

## REFERENCES

-Girault JA, Horiochi A, Gustafson EL, Rosen NL, Greengard P. J Neurosci. 1990 Apr;10(4):1124-33.  
 -Dubouva I, Horiochi A, Snyder GL, Girault JA, Czernik AJ, Shao L, Ramabhadran R, Greengard P, Nairn AC. J Neurochem. 2001 Apr;77(1):225-33.  
 -Mochida S, Maslen SL, Skehel M, Hunt T. Science. 2010 Dec 17;330(6011):1670-3.  
 -Gharby-Ayachi A, Labbé JC, Burgess A, Vigneron S, Strub JM, Broudes E, Van Dorsselaer A, Castro A, Lorca T. Science. 2010 Dec 17;330(6011):1673-7.  
 -Nairn A, Snyder GL, Greengard P. J Neurosci. 1997 Nov 11;17(21):8147-55.

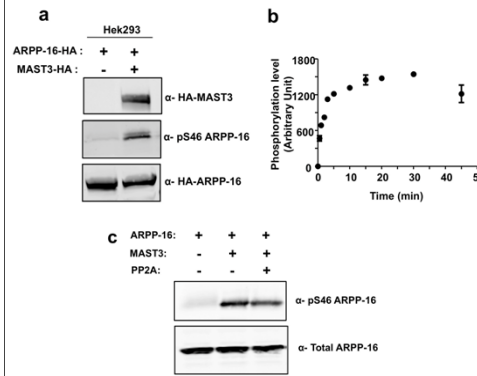
## RESULTS

**Figure 1: Identification of binding partners of ARPP-16 in rodent striatum, ARPP-16 interacts with the A subunit of PP2A.**



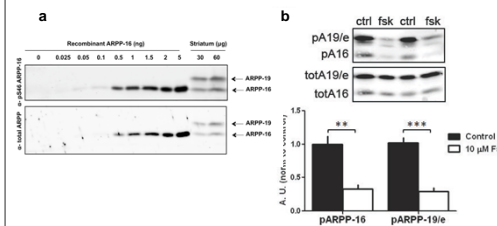
**A.** Rat brain S2 fractions were incubated with immobilized His-ARPP-16, then eluted proteins separated using DIGE. The striatal sample was labeled with Cy2, while the control sample (non-specific binding of striatal samples to beads with no ARPP-16) was labeled with Cy3. Samples were mixed and analyzed by DIGE. The white arrow indicates a spot corresponding to PP2A-A and the arrowhead indicates a spot corresponding to tubulin. **B.** Independent striatal S2 samples were incubated with immobilized His-ARPP-16 (His-A16), and bound proteins were analyzed by SDS-PAGE and immunoblotting with antibodies to PP2A-A (red) and PP2A-C (green). Striatal samples were also bound to beads with no His-ARPP-16 (lanes 1 and 2). **C.** Increasing amounts of recombinant, SEC-purified PP2A-A were incubated with immobilized His-ARPP-16 (His-A16), and bound protein was analyzed by SDS-PAGE and immunoblotting with antibodies to PP2A-A (red) and PP2A-C (green). Striatal samples were also bound to beads with no His-ARPP-16 (lanes 1 and 2). **D.** Full-length GST-PP2A-A, GST-tagged truncation mutants of PP2A-A that included HEAT repeats HEAT1-7, HEAT1-9, or HEAT3-END, or a GST tag control were incubated with immobilized onto Glutathione Sepharose 4 Fast Flow beads and incubated with increasing amounts of recombinant, SEC-purified His-ARPP-16 (A16, 100 nM, 100 nM, or 1000 nM) or SEC-purified His-ARPP-19 (A19, 10 nM, 100 nM, or 1000 nM). Recombinant RCS (100 nM or 1000 nM) was incubated with beads to determine non-specific binding. Eluted samples were analyzed by SDS-PAGE and immunoblotting for ARPP-16 or ARPP-19.

**Figure 2: ARPP-16 is phosphorylated at Ser46 in intact cells and *in vitro* by MAST3 Kinase.**



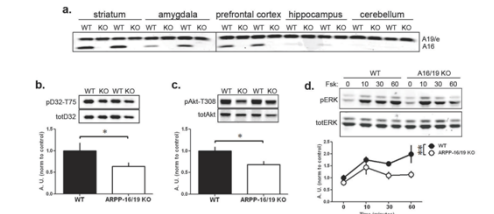
**A.** HEK293 were transfected with HA-ARPP-16 without or with HA-MAST3 kinase and the phosphorylation at Ser46 of ARPP-16 was analyzed by immunoblotting using phospho-specific antibody. **B.** Recombinant purified ARPP-16 (1  $\mu$ M) was incubated with immunoprecipitated MAST3 Kinase for various times (as indicated), and phosphorylation of Ser46 was measured by immunoblotting. Ser-46 phosphorylation was normalized to total ARPP-16 levels, and to the zero time value in each experiment. Results shown represent the average from three experiments. **C.** Prevention of PP2A dephosphorylation of Ser46 in ARPP-16 *in vitro* through use of  $\gamma$ -ATP. Purified HA-ARPP-16 (1  $\mu$ M) was phosphorylated *in vitro* with MAST3 kinase in presence of Thio-ATP. Then P- $\gamma$ -Ser46-ARPP-16 was incubated with PP2A for ten minutes and phosphorylation of Ser46 in ARPP-16 with or without PP2A incubation was measured by immunoblotting. The ability of PP2A to dephosphorylate ARPP-16 is strongly decreased by the phosphorylation of ARPP-16 with Thio-ATP.

**Figure 4: S46 of ARPP-16 is basally phosphorylated to high stoichiometry in striatal slices and is dephosphorylated in response to cAMP signaling**



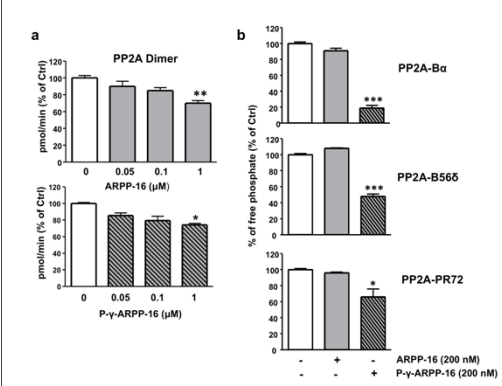
**A.** P-Ser46-ARPP-16 basal levels were assessed in striatum lysates by comparison with increasing amounts of MAST3-phosphorylated recombinant ARPP-16 using a phospho-specific Ser46 Antibody. **B.** Rat striatal slices (n = 6 per condition) were treated without (ctrl, Control) or with 10  $\mu$ M forskolin (fsk) for 0 min or 10 min with continual oxygenation in aCSF. Samples (30  $\mu$ g total lysate) were analyzed by SDS-PAGE and immunoblotting for phospho-S46 and total ARPP-16 or phospho-Ser 62 and total ARPP-19/ENSA (upper panels). Phospho-site signals were each normalized to total protein, and data for forskolin treatment was normalized to controls (lower bar graph); Student's t-test \*p<0.01, \*\*p<0.001.

**Figure 5: ARPP-16 acts to regulate phosphorylation of selective PP2A substrates in striatal neurons**



**A.** Samples from different brain regions (as indicated) from wild-type (WT) and conditional, under CamKII promoter, ARPP-16 knockout (KO) mice were analyzed by SDS-PAGE and immunoblotting with an antibody that recognizes ARPP-16, ARPP-19 and ENSA. Striatal slices from ARPP-16/19-KO or WT littermate controls were isolated and basal phosphorylation of the PP2A targets, **(b)** DARPP-32 at T75 or **(c)** Akt at T308 were analyzed by SDS-PAGE and immunoblotting. Upper panels show (b) phospho-T75 (pD32-T75) and total DARPP-32 (totalD32) or (c) phospho-T308 (pAkt-T308) or total Akt (totalAkt) blots. Lower bar graphs shows cumulative data. **(d)** Student's t-test \*p<0.05, error bars show SEM/SD. **(d)** Striatal slices from ARPP-16/19-KO or WT littermate controls were treated with 10  $\mu$ M forskolin with continual oxygenation in aCSF for 0 min, 10 min, 30 min, or 60 min. Samples were analyzed by SDS-PAGE and immunoblotting for phospho-T202 and total ERK2 (upper panels). Lower graph shows cumulative data (RM-ANOVA, \*\*p<0.01). For b, c and d phospho-site signals were each normalized to total protein, and then data for KO mouse samples was normalized to controls.

**Figure 3: P-S46-ARPP-16 selectively inhibits PP2A heterotrimers in their ability to dephosphorylate P-T75-DARPP-32 *in vitro*.**



**A.** Purified PP2A-AC dimer (0.01  $\mu$ l) was incubated with increasing concentration (0 nM, 50 nM, 100 nM and 1  $\mu$ M) of recombinant, purified ARPP-16 (upper panel) or P- $\gamma$ -Ser46-ARPP-16 (lower panel) for 10 minutes at 37°C with 500  $\mu$ M phosphatase. Phosphate release was detected using a malachite green assay with absorbance at 650 nm. **B.** Recombinant Purified PP2A trimer over-expressed in HEK293 cells and isolated by immunoprecipitation with anti-Flag Ab, were incubated with 200 nM of ARPP-16 or P- $\gamma$ -Ser46-ARPP-16 for 10 minutes at 37°C with P- $\gamma$ -T75-DARPP32. The ability of different PP2A trimers to dephosphorylate DARPP32 has been measured by scintillation. Results are expressed as percent changes with respect to PP2A alone (white bar). \*, p < 0.05; \*\*, p < 0.01; \*\*\*, p < 0.001, Newman-Keuls' multiple comparison test.

## CONCLUSIONS

- ARPP-16 directly interact with PP2A-A subunit,
- MAST3 kinase phosphorylates ARPP-16 on Ser46 site,
- Phospho-ARPP-16/19 negatively regulates PP2A activity, when the enzyme is in the trimeric form,
- Phospho-ARPP-16 inhibits PP2A ability to dephosphorylate DARPP-32 on Thr75, and showed a variable specificity for different PP2A heterotrimers,
- The phosphorylation of ARPP-16/19 on MAST3 site is high under basal conditions in mouse striatum and decrease following stimulation of adenylyl cyclase by forskolin,
- KO mice for ARPP-16/19 in striatum showed a significant decrease in the phosphorylation level of specific PP2A targets such as T75-DARPP32, Akt and MAPK/Erk.

## ACKNOWLEDGMENTS

This research was funded by NIDA (XXX). MAST constructs were kindly provided by Rafael Pulido.